Quantifying Mineral Surface Energy by Scanning Force Microscopy

Bastian Sauerer,[1] Mikhail Stukan,[2] Wael Abdallah,[1]* Maryam H. Derkani,[3] Maxim Fedorov,[4] Jan Buiting,[5] Zhenyu J. Zhang[3¶]*

[1]*Schlumberger Middle East, S.A., Schlumberger Dhahran Carbonate Research Center, Dhahran Techno Valley, P.O. Box 39011, Dammam 31942, Saudi Arabia*

[2]*Schlumberger Moscow Research, Pudovkina 13, Moscow 119285, Russia*

[3]*Department of Chemical & Process Engineering, University of Strathclyde, Montrose Street, Glasgow, UK, G1 1XJ*

[4]*Department of Physics, Scottish Universities Physics Alliance (SUPA), University of Strathclyde, 107 Rottenrow East, Glasgow, UK, G4 0NG*

[5]*Retired, formerly from Saudi ARAMCO, Reservoir Characterization Department, Dhahran 31311, Saudi Arabia*

[¶]*Current address: School of Chemical Engineering, University of Birmingham, Edgbaston, Birmingham, UK, B15 2TT*

KEYWORDS: calcite, dolomite, surface energy, wettability, SFM

ABSTRACT: Fundamental understanding of the wettability of carbonate formations can potentially be applied to the development of oil recovery strategies in a complex carbonate reservoir. In the present study, surface energies of representative carbonate samples were evaluated by direct quantitative force measurements, using scanning force microscopy (SFM) at sub-micron scale, to develop a reliable method to predict reservoir wettability. Local adhesion force measurements were conducted on appropriate calcite and dolomite samples and performed in air as well as in the presence of polar and nonpolar fluids. This study demonstrated that, by comparing measurements of adhesion forces between samples of the same mineral in different fluids, it is feasible to determine the surface energy of a given mineral as well as its polar and nonpolar components. The derived values are in agreement with literature. A proof-of-principle protocol has been established to quantify surface energy using SFM-based adhesion measurements. This novel methodology complements the conventional contact angle measurement technique, where surface energy can only be examined at large length scale. The reported methodology has great potential for further optimization into a new standard method for fast and accurate surface energy determination, and hence provides a new tool for reservoir rock wettability characterization.

INTRODUCTION

Understanding characteristics of reservoir rocks, reservoir fluids and the interaction between them is the basis of reservoir characterization. For example, at the primary production design stage, it is crucial to understand the relative permeability and capillary pressure to determine the fluid flow patterns that will be implemented to control oil production. When planning a secondary or tertiary production strategy, it is critical to re-evaluate the same parameters. As such, fluids interfacial tension and reservoir rock wettability are two critical parameters for any reservoir characterization to be used for production design which includes estimating reserves and recovery factor.

Wettability of reservoir rocks has a strong influence on the amount of recoverable oil because a water-wet mineral surface is beneficial when oil is recovered by water flooding.[1] In this case, water imbibition into pores is supported by the positive capillary pressure, which improves the oil recovery. It is widely accepted that carbonate rock formations are moderately to strongly oil-wet.[2, 3] This is attributed to the adsorption of polar compounds contained in crude oil such as carboxylic acids and asphaltenes, onto the carbonate surface, which results in the rock surface changing from hydrophilic to hydrophobic.[2, 4] Consequently, oil relative permeability is lower and displacement efficiency is poor. To achieve better oil recovery rates, it is highly desirable to: (i) acquire a fundamental understanding of the actual carbonate reservoir wettability, (ii) evaluate the role of reservoir fluids on surface wettability, and (iii) predict reservoir wettability using surface energy measurements.

Several techniques are available for reservoir wettability measurements; these include imbibition and centrifuge capillary pressure, which are done on reservoir core plugs.[5] Industry standard techniques, e.g. the Amott-Harvey imbibition test and the U. S. Bureau of Mines method, suffer from sample alteration and fluid loss during the coring operation and transport to the laboratory and therefore do not necessarily provide an accurate reservoir wettability. Another technique to determine wettability is the contact angle measurement, which is based on monitoring the contact angle between (at least) three different liquids (with known surface tension components) and the sample surface. This approach requires a smooth, flat and nonporous rock surface on which a droplet of test liquid is placed. However, all reservoir rocks are porous, so contact angle measurements can only provide qualitative results. Therefore, currently there is no suitable and reliable technique for measuring a quantitatively accurate wettability.

Despite the extensive theoretical and experimental work performed in the past few decades, surface energy of solids is still a matter of ongoing debate. The approach proposed by van Oss and coworkers,[6-8] known as the van-Oss-Chaudhury-Good theory (vOCG), has been used widely in the oil industry. According to this theory, surface interactions are split into two components: Lifshitz-van der Waals (LW) forces (that include London dispersion forces, Debye induction, and Keesom orientation forces where dispersion forces are the main component) and another group of forces that originate from electron donor-acceptor (Lewis acid-base, AB) interactions. By resolving the equations developed from the van Oss model, the surface energy of a solid surface can be calculated as well as its polar and nonpolar components. A great advantage of this approach is accessing information about the acid-base properties of a given surface by measuring its contact angle with various test liquids. Although this method being widely applied as documented in the literature, numerous drawbacks of this approach have been reported[9-12]: (i) there is a lack of a broad spectrum of test liquids that are well characterized; although there are adequate choices for basic liquids, there are only limited choices for predominantly acidic liquids; (ii) inconsistent surface energy components are obtained when using different sets of liquid tests; (iii) surface energy measured by contact angle measurements depends strongly on surface and environmental conditions.

In a previous study[13] the vOCG approach was used to interpret the surface energy components of calcite and dolomite based on contact angle measurements. The results showed that the surface energy components are dependent on the selected polar probe liquid and the surface characteristics, e.g. roughness and cleanliness. The dispersive surface energy component can be calculated with a high confidence level whereas the polar component calculation was less consistent. Using a probe fluid triplet of 1-bromonaphthalene/water/formamide (B/W/F), the total surface energy of calcite and dolo-

mite were estimated as 58.2 ±1.5 mN/m and 58.1 ±0.8 mN/m respectively. At the same time, according to measurements performed using a 1-bromonaphthalene/water/ethylene glycol (B/W/E) fluid triplet, dolomite has slightly higher total surface energy, 59.4 ±1.4 mN/m, compared to the previous system, whereas that of calcite decreased to 44.2 ±0.2 mN/m. These results, summarized in Table 1, are within the range of published values.[14-16]

One of the major benefits in measuring solid surface energy directly is that it provides the true surface tension in the presence of liquid and facilitates accurate prediction of rock wettability. However, since inconsistent values of surface energy components were reported in the literature, it is crucial to examine whether the roots of inconsistency are related to the fluids used, the surface conditions or the technique being used.

When exposed to organic solvents, surface dissolution is no longer an issue for calcite; however, the volatility and viscosity of the solvents pose additional technical challenges to contact angle experiments. An alternative approach is using scanning force microscopy (SFM), a direct quantitative measurement, to determine surface energy. By quantifying the force needed to detach two surfaces in contact, the surface energy can be calculated based on the contact geometry.

Table 1. Calculated surface energy by components based on contact angle measurements for calcite and dolomite using the van Oss method[9,10] and compared to reported data in the literature. All values are in mN/m.

Mineral	γ^+_s	γ^-_s	γ_s^{AB}	γ_s^{LW}	γ_s^{TOT}	Ref.
Calcite	3.2	39.3	22.3	35.8	58.2	B/W/F[13]
	0.6	27.9	8.3	35.8	44.2	B/W/E[13]
	0.8	58.8	14.1	42.2	56.3	[14]
	0.1	29.0	2.8	43.8	46.7	[15]
	1.3	54.4	16.8	40.2	57.0	[16]
Dolomite	1.3	57.9	17.2	40.9	58.1	B/W/F[13]
	1.4	59.0	18.4	40.9	59.4	B/W/E[13]
	1.9	33.3	15.9	43.5	59.4	[14]
	0.2	30.5	4.9	37.6	42.5	[16]

The major objective of this work is to develop a new methodology, based on SFM, to quantify the total surface energy and the respective contributing polar and nonpolar components for typical reservoir minerals. The adhesion forces measured by SFM can be used to calculate surface energy components. The advantages of SFM over the conventional methods, are that it not only provides surface topography with a molecular scale resolution, but also measures adhesion forces acting at the tip-sample interface. Various operational principles are described and reviewed extensively in the literature.[17-20] SFM adhesion force measurements in the oil industry are limited due to the challenges posed by variations caused by heterogeneity of the sample and characteristics of the tip.[21] It was also reported that surface roughness could result in uncertainties in determining surface adhesion force.[22, 23]

Measurements of colloidal interactions between particles and the surface were described in the literature, e.g. interactions of drug molecules with the surface material of their canisters in pharmaceutical research[24] or forces between bacterial cells and solid substrates for biomaterial development.[25, 26] Although commercially available cantilevers or particle-attached probes have been widely used to compare the difference in adhesion for various materials, no SFM force measurement has been done with a calcite or dolomite particle attached directly to an SFM cantilever. This is because an undefined geometry of a natural calcite or dolomite particle will result in unrepeatable measurements. To overcome this challenge, a new fabrication methodology for calcite and dolomite particles was employed to facilitate the measurement of the adhesion force between the same carbonate formation materials, hence providing a more accurate value of surface energy.

THEORETICAL BACKGROUND

Adhesion force (F_{adh}) between the tip (micro-particle attached to an SFM cantilever) and the substrate, also known as pull-off force ($F_{pull\text{-}off}$), is not directly linked to the value of the work of adhesion per unit area (W_{adh}). With the assumption of a spherical probe contacting a flat surface this link can be established[19] using the contact mechanics theory developed in 1971 by Johnson, Kendall and Roberts (JKR)[27]:

$$F_{adh} = 1.5\pi R W_{adh} \quad (1)$$

for compliant materials with high surface energy, and large micro particles (radius R in the μm range). The contacting bodies are assumed to be in adhesional contact, and are considered to be elastic; viscoelasticity is not taken into account.

The work of adhesion W_{adh} per unit area between surfaces of two flat and identical solids (i) can be expressed in terms of surface tension, γ_i, when interacting in air:

$$W_{ii} = 2\gamma_i \quad (2)$$

For two dissimilar surfaces (i, j) in air, the work of adhesion per unit area is defined as

$$W_{ij} = \gamma_i + \gamma_j - \gamma_{ij} \quad (3)$$

or

$$W_{ikj} = \gamma_{ik} + \gamma_{jk} - \gamma_{ij} \quad (4)$$

if the surfaces are interacting in a medium k.

A commonly used approach to treat solid surface tension is to express it as the sum of components associated with dispersion forces (γ^{LW}) and acid-base interactions (γ^{AB})[28], as was suggested by van Oss et al.[6]:

$$\gamma = \gamma^{LW} + \gamma^{AB} \quad (5)$$

For Lifshitz-van der Waals interactions between two media i and j the Good-Girifalco-Fowkes combining rule[29] is applicable:

$$\gamma_{ij}^{LW} = \left(\sqrt{\gamma_i^{LW}} - \sqrt{\gamma_j^{LW}}\right)^2 \quad (6)$$

Unlike γ^{LW}, the Lifshitz-van der Waals component, the acid-base component γ^{AB} comprises two non-additive parameters (γ^+, γ^-):

$$\gamma^{AB} = 2\sqrt{\gamma^+ . \gamma^-} \quad (7)$$

These acid-base interactions are complementary in nature, and are the electron-acceptor surface tension parameter and the electron-donor surface tension parameter. The acid-base component of the interfacial tension between two solid surfaces i and j is written then as[6]

$$\gamma_{ij}^{AB} = 2\left(\sqrt{\gamma_i^+} - \sqrt{\gamma_j^+}\right)\left(\sqrt{\gamma_i^-} - \sqrt{\gamma_j^-}\right) \quad (8)$$

The total interfacial tension between two phases is then formulated as

$$\gamma_{ij} = \gamma_{ij}^{LW} + \gamma_{ij}^{AB} = \left(\sqrt{\gamma_i^{LW}} - \sqrt{\gamma_j^{LW}}\right)^2 + 2\left(\sqrt{\gamma_i^+} - \sqrt{\gamma_j^+}\right)\left(\sqrt{\gamma_i^-} - \sqrt{\gamma_j^-}\right) \quad (9)$$

Application to carbonate surfaces. To determine surface energy components of carbonate formations accurately from SFM measurements, a fabricated carbonate crystal was mounted at the cantilever tip and adhesion force measurements were performed between two carbonate surfaces in different media. Using Eq. (1) corresponding surface energies per unit area were calculated for each system considered.

Nonpolar surface energy. According to Eq. (4), surface energy per unit area between two carbonate surfaces interacting in a nonpolar fluid (fl) can be formulated as

$$W_{cf1c} = 2\gamma_{cf1} \quad (10)$$

where c and f1 represent carbonate and nonpolar fluid 1, respectively. Taking into account Eq. (9), work of adhesion per unit area is written as

$$W_{cf1c} = 2\left(\gamma_{cf1}^{LW} + \gamma_{cf1}^{AB}\right) = 2\left(\left[\gamma_c^{LW} + \gamma_{f1}^{LW} - 2\sqrt{\gamma_c^{LW}.\gamma_{f1}^{LW}}\right] + 2\sqrt{\gamma_c^+.\gamma_c^-}\right) \quad (11)$$

where $(\gamma_{f1}^+ = \gamma_{f1}^- = 0)$ since the fluid is nonpolar.

Likewise for a nonpolar fluid 2 (f2), work of adhesion per unit area of carbonate probe/carbonate surface is written as:

$$W_{cf2c} = 2\left(\left[\gamma_c^{LW} + \gamma_{f2}^{LW} - 2\sqrt{\gamma_c^{LW}.\gamma_{f2}^{LW}}\right] + 2\sqrt{\gamma_c^+.\gamma_c^-}\right) \quad (12)$$

where $(\gamma_{f2}^+ = \gamma_{f2}^- = 0)$

Subtracting Eq. (12) from Eq. (11) will result in

$$\frac{1}{2}(W_{cf1c} - W_{cf2c}) = \left(\gamma_{f1}^{LW} - \gamma_{f2}^{LW}\right) - 2\sqrt{\gamma_c^{LW}}\left[\sqrt{\gamma_{f1}^{LW}} - \sqrt{\gamma_{f2}^{LW}}\right] \quad (13)$$

From Eq. (13), γ_c^{LW} can be deduced with the following expression:

$$\gamma_c^{LW} = \left(\frac{\left(\gamma_{f1}^{LW} - \gamma_{f2}^{LW}\right) - \frac{\left(W_{cf1c} - W_{cf2c}\right)}{2}}{2\left(\sqrt{\gamma_{f1}^{LW}} - \sqrt{\gamma_{f2}^{LW}}\right)}\right)^2 \quad (14)$$

Polar surface energy To calculate polar components of carbonate surface energy, both polar and nonpolar fluids should be used to extract γ_c^+ and γ_c^- from adhesion data collected by SFM.

In the case of two carbonate surfaces in a polar fluid (f3), work of adhesion per unit area is written as:

$$W_{cf3c} = 2\left(\gamma_{cf3}^{LW} + 2\sqrt{\gamma_c^+.\gamma_c^-} - 2\sqrt{\gamma_c^+.\gamma_{f3}^-} - 2\sqrt{\gamma_c^-.\gamma_{f3}^+} + 2\sqrt{\gamma_{f3}^+.\gamma_{f3}^-}\right) \quad (15)$$

To calculate acid-polar and base-polar surface energy components for carbonates, we solve a system of linear equations with two unknowns by substitution method. Subtracting Eq. (15) from Eq. (11) we get

$$\sqrt{\gamma_c^+.\gamma_{f3}^-} + \sqrt{\gamma_c^-.\gamma_{f3}^+} = A \quad (16)$$

where

$$A = 0.25\left(W_{cf1c} - W_{cf3c} - 2\gamma_{cf1}^{LW} + 2\gamma_{cf3}^{LW} + 4\sqrt{\gamma_{f3}^+.\gamma_{f3}^-}\right) \quad (17)$$

Eq. (11) can be written as

$$\sqrt{\gamma_c^+.\gamma_c^-} = \frac{W_{cf1c} - 2\gamma_{cf1}^{LW}}{4} = B \quad (18)$$

Replacing $\sqrt{\gamma_c^+}$ from Eq. (18) into Eq. (16) results in

$$\left(\sqrt{\gamma_c^-} - C\right)^2 = D \quad (19)$$

where $C = \frac{A}{2\sqrt{\gamma_{f3}^+}}$ and $D = \frac{A^2}{4\gamma_{f3}^+} - \frac{B\sqrt{\gamma_{f3}^-}}{\sqrt{\gamma_{f3}^+}}$

Since all surface tension components for liquids are supposed to be known, and Lifshitz-van der Waals components γ_{cf1}^{LW} and γ_{cf3}^{LW} are obtained using Eqs. (14) and (6), Eq. (19) can be resolved with respect to γ_c^-, whereas γ_c^+ can be then calculated using Eq. (18).

Once γ_c^- and γ_c^+ are known, γ_c^{AB} can be calculated as

$$\gamma_c^{AB} = 2\sqrt{\gamma_c^+ \cdot \gamma_c^-} \quad (20)$$

To calculate surface wettability, the Young-Dupré equation

$$\cos\theta = \frac{\gamma_{cf1} - \gamma_{cf2}}{\gamma_{f1f2}} \quad (21)$$

can be used, where the surface wettability is represented by contact angle θ.

Overall workflow. Figure 1 presents the proposed scheme to calculate reservoir rock surface energy and wettability for any given solid (s) using different fluids (f).

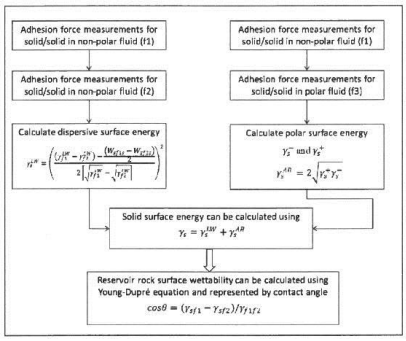

Figure 1. Flow chart describing the required measurements and calculations for determination of solid surface energy and wettability.[30]

EXPERIMENTAL SECTION

Materials. Ethylene glycol (99.8% purity), 1-bromonaphthalene (97% purity), and heptane (99% purity), used as polar and nonpolar test fluids respectively, were purchased from Sigma-Aldrich (Dorset, UK) and used as received.

Fabrication of cantilever. Customized particle probes were manufactured by Novascan Technologies Inc. (Ames, IA, USA). The received cantilevers were made from silicon nitride with mineral particle attached to the end (average nominal spring constant of 0.35 N/m). Calcite (46 E 1436, Iceland Spar, Creel, Chihuahua, Mexico) and dolomite (46 E 2718, Butte, Montana, USA) were purchased from Ward's Natural Science and used as cleaved crystals for the samples and for probe manufacturing.

Hemispherical structures of 4 μm diameter were fabricated on calcite and dolomite particles fixed at the end of the SFM cantilever using focused ion beam (FIB) machining. The experiment was carried out on a FEI Quanta 3D FEG dual beam system equipped with a field emission scanning electron microscope (SEM) and a liquid gallium (Ga^+) ion source.

FIB experimental procedures are illustrated in Figure 2. After the top surface was polished with a given current, a divergence compensation method[31] was applied. After 1103 scanning passes for dolomite and 752 passes for calcite, hemispheres with 4 μm diameter were obtained. The ion beam was then redirected to the edge of the particle to remove any residual material around the hemisphere.

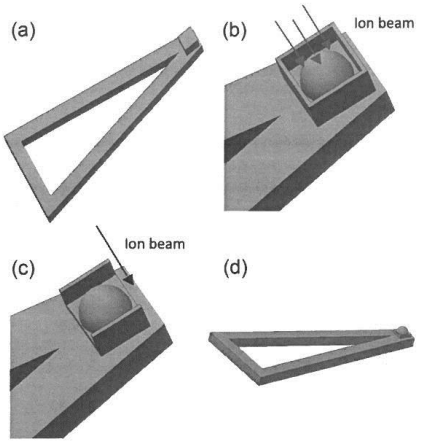

Figure 2. Schematic diagrams showing the FIB machining process: (a) customized particle probe before fabrication, (b) hemispherical geometry fabrication, (c) removal of residual material, (d) SFM cantilever after fabrication.

Force measurements. A molecular force probe (MFP-3D, Asylum Research) equipped with a liquid cell was employed for force measurements. The experiments were carried out by submerging the fabricated calcite or dolomite cantilever in the selected liquid at room temperature. The spring constant of each SFM cantilever was calibrated in the same solution prior to any force measurements using the built-in thermal fluctuation method.[32] The approach speed of the cantilever was 1 μm/s and the pulling distance was 1 μm with no dwell time allowed. Applied force was kept at 2 nN throughout the measurements. Force measurements were repeated three times for each combination of solid and liquid from which over 500 force curves were collected.

In general, SFM force measurements can provide a range of important surface properties, including attractive and repulsive forces at the interface. Furthermore, the contact area between tip and sample, as well as sample plasticity and elastic modulus can be obtained. Different contact mechanics theories, discussed in literature, can be used to describe the contact area. To choose the most suitable one, the chemical and mechanical properties of the tip and the sample need to be assessed.

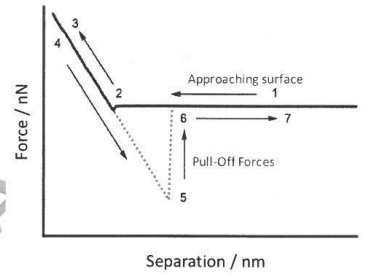

Figure 3. A representative force curve acquired between the calcite tip and the calcite sample in 1-bromonaphthalene. The solid curve represents the approaching part and the dotted curve represents the retraction part. Arrows indicate the chronological sequence of one measurement cycle.

A representative force curve collected by a calcite tip on a calcite sample is shown in Figure 3. At the beginning of a typical force measurement cycle, the SFM cantilever is kept away from the sample, and

the cantilever remains in a non-interacting equilibrium state (point 1); hence, no surface interaction is involved. Separation (in the z direction) decreases as the tip is brought closer to the sample at a constant speed. Once the tip is close enough to the sample surface, attractive surface forces overcome the stiffness of the cantilever, causing the tip to jump into contact with the sample surface (point 2). The cantilever continues to move towards the sample, resulting in a gradual bending of the cantilever (point 3) until such movement is stopped (point 4). These points comprise the approach part (solid curve in Figure 3). As the cantilever starts to move away from the sample, the retraction part (dotted curve in Figure 3) is recorded (points 4-5). Due to the adhesion formed, the tip remains in contact with the sample surface until the adhesion forces are overcome, leading to a sharp transition to the noncontact position (points 5-6). After that, tip-sample separation increases again without influence on the deflection (points 6-7). With the calibrated spring constant and deflection sensitivity for each cantilever, these force measurements allow a direct reading of the adhesion force from the retraction part of the curve.

RESULTS AND DISCUSSION

Cantilever fabrication. Initially, the calcite and dolomite particles glued to the SFM cantilevers did not have a defined shape; hence, the FIB technique was employed so that a desired geometry could be fabricated. To ensure a consistent contact area, a key factor guaranteeing repeatability, hemispherical geometry was chosen. Figure 4 presents SEM images acquired during the FIB procedure in which a calcite particle of irregular shape was processed. As described in the experimental section, the top surface was polished before the desired structure could be generated. The finished geometry was a hemisphere of 4 μm diameter which is confirmed by the SEM images shown in Figures 4 and 5.

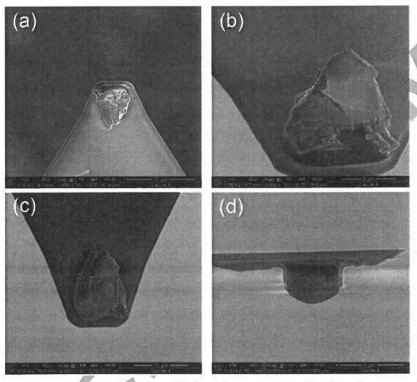

Figure 4. SEM images of (a) calcite particle fixed on an SFM cantilever, (b) top surface after polishing, (c) hemispherical geometry fabricated in the calcite particle, (d) calcite probe in the final shape.

Using the FIB method, a number of calcite and dolomite tips were processed to generate hemispheric structures of 4 μm diameter. Representative SEM images of those tips are shown in Figure 5. A great level of consistency was maintained across different probes even though they had irregular shape and thickness initially. The determined tip radius (2 μm) was used in the contact mechanics calculation and surface energy estimation.

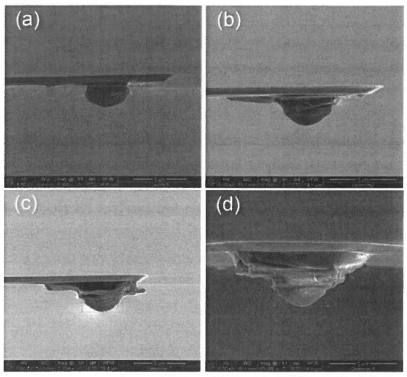

Figure 5. Representative SEM images of hemispherical calcite (a) and dolomite (b-d) probes produced by the FIB procedure.

Adhesion measurements in ambient conditions. To avoid cross-contamination from one test fluid to another, each tip was assigned to a specific liquid. The advantage of such rigorous protocol is to prevent any potential tip surface alteration during washing steps. However, to compare data collected by different probes, it is vitally important to implement measurements in ambient conditions as control experiments. The additional advantage of this step is to eliminate any potential inconsistency between different SFM cantilevers because the size of the contact area between probe and mineral substrate is the key parameter to link adhesion force and work of adhesion.

All of the calcite and dolomite tips were tested in ambient conditions against the corresponding mineral sample before they were exposed to specific solvents. Figure 6 shows a representative histogram of adhesion force between a dolomite tip and a dolomite sample obtained in ambient conditions. The distribution of adhesion force, represented by the number of events, is within the range of 5 to 15 nN. The relatively wide distribution of adhesion force, also shown in Figures 7 and 8, is attributed to the high degree of heterogeneity on the mineral surface.

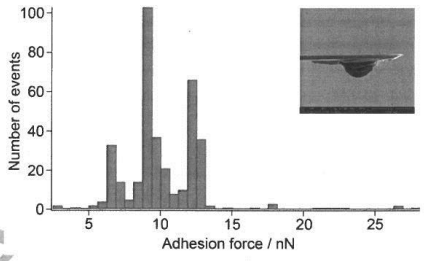

Figure 6. Representative histogram of adhesion force between dolomite tip and dolomite surface in ambient conditions.

Adhesion measurements in liquid. Once a tip was tested in ambient conditions and its surface adhesion fell in the expected range, the tip was used to measure surface adhesion in a selected fluid. Three solvents, ethylene glycol, 1-bromonaphthalene, and heptane were chosen to represent polar and nonpolar liquids. For each pair of experimental carbonate models, calcite-calcite or dolomite-dolomite, adhesion measurements were performed in all three solvents respectively. Representative force curves collected for all systems investigated are presented in the Supporting Material. Figure 7 presents statis-

tical histograms of adhesion force between dolomite tips and dolomite samples. The result shows that all three solvents facilitate a reduction in surface adhesion forces, compared to those acquired in ambient conditions, which is consistent with theory. The averaged adhesion forces for each solvent are summarized in Table 2. Adhesion between dolomite and dolomite is very close in heptane and 1-bromonaphthalene, but becomes slightly greater in ethylene glycol.

It was also noticed that the adhesion forces measured in all cases (polar and nonpolar solvents) were reduced to a great extent to less than 1 nN. This could either be due to an excessive masking of the surface forces by the solvents, or to an overestimation of the values measured in ambient conditions, which can be intensified by water layers on the dolomite. Corresponding adhesion force for each combination of dolomite tip and dolomite sample, acquired in ambient conditions, is presented as inset in Figure 7. Similar to the data in Figure 6, distribution of adhesion force in ambient conditions spreads over a wide range, up to 40 nN, which is consistent with a recent work in which adhesion force between microparticle and solid substrate was quantified by SFM.[33]

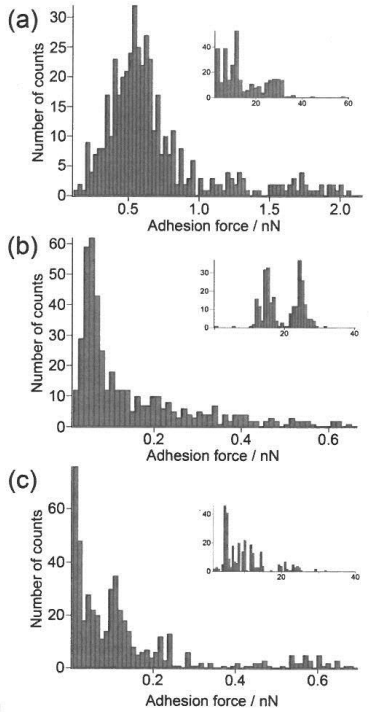

Figure 7. Histograms of adhesion force between a dolomite tip and a dolomite sample in three different solvents (a) ethylene glycol, (b) 1-bromonaphthalene, and (c) heptane, based on multiple SFM measurements. Adhesion data acquired in ambient conditions for the corresponding cantilevers are presented as insets.

The same protocol was performed with a new pair of calcite tip and calcite sample for each of the three solvents, following the respective force measurements in ambient conditions. Histograms of adhesion force for the calcite-calcite contact are presented in Figure 8. Similar to that for the dolomite probes, the adhesion force in solvents is significantly lower than that in ambient conditions. This is not surprising since the adhesion acquired on calcite is less than 500 pN when a standard SFM cantilever

was used in a previous study.[34] Even though there are a significant number of step edges, imperfections, and impurities on natural calcite, the discrepancy between adhesion forces acquired in ambient conditions is reduced substantially in all three liquids. The adhesion force between calcite surfaces is found to be greater than that between dolomite surfaces, for all three solvents. For the calcite system, the minimum adhesion force was obtained in heptane, the maximum one in 1-bromonaphthalene.

It is worth noting that the adhesion force acquired between calcite and calcite in ambient conditions is generally greater than that between dolomite and dolomite. Although it is widely accepted that a layer of water of a few angstroms thick adsorbs on mineral surfaces,[35] calcite appears to have a particularly strong affinity for water, as a 1.7 nm water layer was observed on calcite surfaces with relatively low humidity.[36]

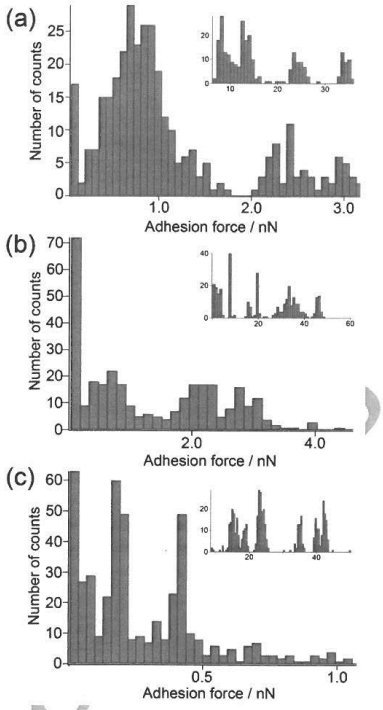

Figure 8. Histograms of adhesion force between calcite tip and calcite sample in three different solvents (a) ethylene glycol, (b) 1-bromonaphthalene, and (c) heptane, based on multiple SFM measurements. Adhesion data acquired in ambient conditions for the corresponding cantilevers are presented in the insets.

Surface energy calculation. Using the average values for the measured adhesion forces for the systems of calcite and dolomite in the respective fluids (Table 2), we were able to calculate polar and nonpolar components, as well as the total surface energy of these minerals applying the theory and the derived formulas described in the Theoretical Background section. The measured force was converted to work of adhesion using a radius of 2 μm and the JKR model applying Eq. (1).

Table 2. Averaged adhesion force and calculated work of adhesion per unit area measured on the carbonate formation minerals in respective solvents.

Mineral	Fluid	F_{adh} [nN]	W_{adh} [mN/m]
Calcite	Ethylene glycol	1.21	0.129
	1-bromonaphthalene	2.27	0.240
	Heptane	0.567	0.060
Dolomite	Ethylene glycol	0.842	0.089
	1-bromonaphthalene	0.155	0.016
	Heptane	0.138	0.015

Using the literature values related to the test fluids (summarized in Table 3), we were able to derive the nonpolar contribution using Eq. (14), the polar contribution from Eqs. (18), (19) and (20), and the total surface energy according to Eq. (5) for both tested minerals (Table 4).

Table 3. Surface tension values of the utilized test liquids in mN/m.

Fluid	γ^{LW} [mN/m]	γ^{+} [mN/m]	γ^{-} [mN/m]
Ethylene glycol	29.0	1.92	47.0
1-bromonaphthalene	44.4	0	0
Heptane	20.1	0	0

Table 4. Nonpolar and polar components as well as total surface energy of the tested minerals.

Mineral	γ^{LW} [mN/m]	γ^{AB} [mN/m]	γ^{tot} [mN/m]
Calcite	30.9	1.11	32.0
Dolomite	31.1	1.18	32.3

Results from experimental measurements using the JKR contact mechanics model for calculation of surface energy values, are shown in Table 4. Although the calculated values of surface energy for dolomite and calcite based on SFM are close to each other, they are lower than those measured previously in the framework of the van Oss decomposition theory and the cited literature (see Table 1). However, surface energy values for carbonate materials reported in the literature show a very broad variation and also depend on the amount of adsorbed water molecules.[37-39] The data confirm that the dispersion energy (γ_s^{LW}) is the major contribution to the total surface energy, compared to the polar acid-base components (γ_s^{AB}). Most of the discrepancy in total surface energy for these minerals is due to variation in the polar energy components, more precisely, all those surfaces are monopolar (more γ_s^- than γ_s^+). Variation of surface energy of the polar component to the dispersion part indicates that surface roughness and heterogeneity has a significant influence on the acid-base interaction. Therefore, it would be chal-

lenging to have good repeatability if similar surface conditions cannot be reproduced. This issue could also have implications for the measured surface forces for the nonpolar solvents. The influence of surface roughness and heterogeneity on the force measurement result was also reported previously.[34, 40] Furthermore, humidity is another factor contributing to decreased surface energy components of minerals because water molecules can adsorb or hydrate the mineral surface and potentially form one or more water layers on the surface.[41-43] Recent computer simulation results suggest that water molecules could strongly bind to calcite surfaces, and dissociation is generally energetically unfavorable.[44] Therefore, this could be one of the reasons why we have a broad distribution of measured adhesion forces in the present study.

The methodology developed in the present study, using carbonate crystals mounted on an SFM cantilever and carbonate surfaces as a substrate, enables direct quantification of adhesion forces, which are dependent on the polarity of the liquid medium. These measurements are sensitive to the environmental conditions and require a large amount of data to ensure good repeatability. The inherent heterogeneity of carbonate samples, despite the use of calcite and dolomite models, is another factor influencing the statistics. Nevertheless, derived total surface energies and the polar and nonpolar components of the tested samples are within the range of values reported in the literature (see Table 4 and Table 1).

CONCLUSION

Instead of contact angle measurements that are widely employed, this study demonstrated that, by direct measurement of adhesion forces between mineral surface and probe of the same mineral, it is possible to acquire complete information about its surface energy decomposition, hence, obtaining polar and nonpolar components. Unlike conventional force measurements where readily available spherical colloids are used exclusively, nanofabrication approach was introduced to consistently produce hemispherical geometry on carbonate formation of irregular shape, which facilitated direct quantification of the interaction between mineral surfaces. The advance in colloidal probe preparation can be employed in a broad spectrum of colloidal systems where interfacial interactions will be measured directly.

This study concludes a proof of principle for the general applicability of the approach based on measurements of adhesion forces by SFM. The novel and unique methodology can be used as an alternative to traditional contact angle measurements in examining surface energy with nanometre spatial resolution. This protocol has great potential for further optimization into a new industrial standard method for fast and accurate surface energy determination, hence providing a new tool for a wide range of applications including reservoir rock characterization and on-line cleaning for chemical processing.

It is important to control surface conditions for the future development of a more robust approach. Similar to contact angle measurements, this SFM method relies strongly on the utilized test liquids. These solvents need to be carefully chosen with regard to the tested solid material of interest to make sure that the masking of force components takes place in the right intensity for further analysis and calculation. As a consequence of the heterogeneous surface composition of natural carbonate formation, adhesion force acquired could have a wide distribution, which can be resolved by increasing number of measurements.

AUTHOR INFORMATION

Corresponding Author

* E-mail: WAbdallah@slb.com; z.j.zhang@bham.ac.uk

Notes

The authors declare no competing financial interest.

ACKNOWLEDGMENTS

The authors would like to express their appreciation to Schlumberger and Saudi Aramco for permission to publish this paper. We also thank Dr Jining Sun from Heriot-Watt University for his assistance with SFM cantilever tip shaping.

REFERENCES

1. Morrow, N.; Buckley, J. Improved oil recovery by low-salinity waterflooding. J. Pet. Technol., 2011, 63, 106-112.
2. Jabbar, M. Y.; Al-Hashim, H. S.; Abdallah, W. Effect of brine composition on wettability alteration of carbonate rocks in the presence of polar compounds. SPE Saudi Arabia Section Annual Technical Symposium and Exhibition, Khobar, Saudi Arabia, 2013, SPE 168067.
3. Abdallah, W.; Gmira, A. Wettability assessment and surface compositional analysis of aged calcite treated with dynamic water. Energy Fuels, 2014, 28, 1652-1663.
4. Batina, N.; Manzano-Martinez, J. C.; Andersen, S. I.; Lira-Galeana, C. AFM characterization of organic deposits on metal substrates from Mexican crude oils. Energy Fuels, 2003, 17, 532–542.
5. Abdallah, W.; Buckley, J.; Carnegie, A.; Edwards, J.; Herold, B.; Fordham, E.; Graue, A.; Habashy, T.; Seleznev, N.; Signer, C.; Hussain, H.; Montaron, B.; Ziauddin, M. Fundamentals of wettability. Oilfield Rev., 2007, 19, 44-61.
6. van Oss, C.; Good, R.; Chaudhury, M. Additive and nonadditive surface tension components and the interpretation of contact angles. Langmuir, 1988, 4, 884-891.
7. van Oss, C. J.; Chaudhury, M. K.; Good, R. J. Interfacial Lifshitz-van der Waals and polar interactions in macroscopic systems. Chem. Rev., 1988, 88, 927-941.
8. van Oss, C. J.; Good, R. J.; Chaudhury, M. K. The role of van der Waals forces and hydrogen bonds in "hydrophobic interactions" between biopolymers and low energy surfaces. J. Colloid Interface Sci., 1986, 111, 378-390.
9. Kwok, D. Y. The usefulness of the Lifshitz–van der Waals acid–base approach for surface tension components and interfacial tensions. Colloids Surf. A, 1999, 156, 191-200.
10. Kwok, D. Y.; Li, D.; Neumann, A. W. Evaluation of the Lifshitz-van der Waals acid-base approach to determine interfacial tensions. Langmuir, 1994, 10, 1323-1328.
11. Della Volpe, C.; Deimichei, A.; Ricco, T. A multiliquid approach to the surface free energy determination of flame-treated surfaces of rubber-toughened polypropylene. J. Adhesion Sci. Technol, 1998, 12, 1141-1180.
12. Della Volpe, C.; Siboni, S. Acid–base surface free energies of solids and the definition of scales in the Good–van Oss–Chaudhury theory. J. Adhesion Sci. Technol., 2000, 14, 235-272.
13. Sauerer, B.; Stukan, M.; Abdallah, W. Unpublished data.
14. Ryder, J. L. Experimental investigation of the factor affecting the wettability of aquifer materials. University of Michigan, 2007.
15. Bargir, S.; Dunn, S.; Jefferson, B.; Macadam, J.; Parsons, S. The use of contact angle measurements to estimate the adhesion propensity of calcium carbonate to solid substrates in water. Appl. Surf. Sci., 2009, 255, 4873-4879.
16. Wu, W.; Giese, R. F.; van Oss, C. J. Change in surface properties of solids caused by grinding. Powder Technol., 1996, 89, 129-132.
17. Magonov, S. N.; Whangbo, M. H. Surface analysis with STM and AFM. VCH: Weinheim, 1996.
18. Noy, A.; Vezenov, D. V.; Lieber, C. M. Chemical force microscopy. Annu. Rev. Mater. Sci., 1997, 27, 381-422.
19. Colton, R. J.; Engel, A.; Frommer, J. E.; Gaub, H. E.; Gewirth, A. A.; Guckenberger, R.; Rabe, J.; Heckl, W. M.; Parkinson, B. Procedures in scanning probe microscopes. Wiley: Chichester, 1998.
20. Cappella, B.; Dietler, G. Force-distance curves by atomic force microscopy. Surf. Sci. Rep., 1999, 34, 1-3, 5-104.
21. Drelich, J.; Tormoen, G. W.; Beach, E. R.; Mittal, K. L. Determination of solid surfaces tension at the nano-scale using atomic force microscopy. In Contact Angle, Wettability and Adhesion, VSP: Leiden, 2006.
22. Leite, F. L.; Riul, A.; Herrmann, P. S. P. Mapping of adhesion forces on soil minerals in air and water by atomic force spectroscopy (AFS). J. Adhesion Sci. Technol., 2003, 17, 2141-2156.

23. Butt, H.-J.; Cappella, B.; Kappl, M. Force measurements with the atomic force microscope: technique, interpretation and applications. Surf. Sci. Rep., 2005, 59, 1-152.
24. Müller, D. J.; Dufrêne, Y. F. Atomic force microscopy as a multifunctional molecular toolbox in nanobiotechnology. Nature Nanotechnology, 2008, 3, 261-269.
25. Pen, Y.; Zhang, Z. J.; Morales-Garcia, A. L.; Mears, M.; Tarmey, D. S.; Edyvean, R. G.; Banwart, S. A.; Geoghegan, M. Effect of extracellular polymeric substances on the mechanical properties of Rhodococcus. Biochim. Biophys. Acta Biomem, 2015, 1848, 518-526.
26. Razatos, A.; Ong, Y.-L.; Sharma, M.; Georgiou, G. Molecular determinants of bacterial adhesion monitored by atomic force microscopy. Proc. Natl. Acad. Sci., 1998, 95, 11059-11064.
27. Johnson, K. L.; Kendall, K.; Robert, A. D. Surface energy and the contact of elastic solids. Proc. R. Soc. Lond. Ser. A, 1971, 324, 301-313.
28. Fowkes, F. M. Additivity of intermolecular forces at interfaces. I. Determination of the contribution to surface and interfacial tensions of dispersion forces in various liquids. J. Phys. Chem., 1963, 67, 2538-2541.
29. Good, R. J.; Girifalco, L. A. A theory for estimation of surface and interfacial energies. III. Estimation of surface energies of solids from contact angle data. J. Phys. Chem., 1960, 64, 561-565.
30. Gmira, A.; Abdallah, W.; Stukan, M.; Buiting, J. J. Measurement of surface energy components and wettability of reservoir rock utilizing atomic force microscopy, US9110094B2, 2015.
31. Sun, J.; Luo, X.; Ritchie, J. M.; Hrncir, T. A predictive divergence compensation approach for the fabrication of three-dimensional microstructures using focused ion beam machining. Proc. Inst. Mech. Eng. Part B J. Eng. Manuf, 2012, 226, 229-238.
32. Hutter, J.; Bechhoefer, J. Calibration of atomic-force microscope tips. Rev. Sci. Instrum., 1993, 64, 1868-1873.
33. Xu, Q.; Li, M.; Zhang, L.; Niu, J.; Xia, Z. Dynamic adhesion forces between microparticles and substrates in water. Langmuir, 2014, 30, 11103-11109.
34. Karoussi, O.; Hamouda, A. A. Macroscopic and nanoscale study of wettability alteration of oil-wet calcite surface in presence of magnesium and sulfate ions. J. Colloid Interface Sci., 2008, 317, 26-34.
35. Ewing, G. E. Ambient thin film water on insulator surfaces. Chem. Rev., 2006, 106, 1511-1526.
36. Bohr, J.; Wogelius, R. A.; Morris, P. M.; Stipp, S. L. S. Thickness and structure of the water film deposited from vapour on calcite surfaces. Geochim. Cosmochim. Acta, 2010, 74, 5985-5999.
37. Royne, A.; Bisschop, J.; Dysthe, D. K. Experimental investigation of surface energy and subcritical crack growth in calcite. J. Geophys. Res., 2011, 116, B04204, 1-10.
38. Tabrizy, V. A.; Denoyel, R.; Hamouda, A. A. Characterization of wettability alteration of calcite, quartz and kaolinite: surface energy analysis. Colloids Surf., A, 2011, 384, 98-108.
39. Arai, Y. The Preparation of Powder. Chapman & Hall: London, 1996.
40. Karoussi, O.; Skovbjerg, L. L.; Hassenkam, T.; Svane Stipp, S. L.; Hamouda, A. A. AFM study of calcite surface exposed to stearic and heptanoic acids. Colloids Surf. A, 2008, 325, 107-114.
41. de Leeuw, N. H.; Parker, S. C. Atomic simulation on the effect of molecular adsorption of water on the surface structure and energies of calcite surfaces. J. Chem. Soc., Faraday Trans., 1997, 93, 467-475.
42. Kerisit, S.; Parker, S. C.; Harding, J. H. Atomistic simulation of the dissociative adsorption of water on calcite surfaces. J. Phys. Chem. B, 2003, 107, 7676-7682.
43. Geissbühler, P.; Fenter, P.; DiMasi, E.; Srajer, G.; Sorensen, L. B.; Sturchio, N. C. Three-dimensional structure of the calcite–water interface by surface X-ray scattering. Surf. Sci., 2004, 573, 191-203.
44. Lardge, J. S.; Duffy, D. M.; Gillan, M. J.; Watkins, M. Ab initio simulation of the interaction between water and defects on the calcite (101 4) surface. J. Phys. Chem. C, 2010, 114, 2664-2668.

Graphical Abstract